Sergei ALEXANDROV*,Robert GOLDSTEIN**,Nelli TCHIKANOVA***

Limit Load Solution for Tubular T-Joint with Rectangular Cross-Section

* Institute for Problems in Mechanics RAS, 101 Prospect Vernadskogo, Moscow 17526, Russia. Presently with Institute of Materials Research, GKSS Research Centre, Max-Planck Str., D-21502 Geesthacht, Germany.
** Institute for Problems in Mechanics RAS, 101 Prospect Vernadskogo, Moscow 117526, Russia.
***Department of Applied Mechanics, Bauman Moscow State Technical University, 2nd Baumanskaya 5, Moscow 107005, Russia.

Keywords: Rigid-plastic, Limit load, T-joint.

ABSTRACT: Axisymmetric and three dimensional kinematically admissible velocity fields for an incompressible rigid-plastic material is proposed. This velocity field involves two velocity discontinuity surfaces. One is situated between deforming material and motionless rigid material and the other is between deforming material and rigid material moving along the z-axis of a cylindrical coordinate system. These velocity discontinuity surfaces form circles on any meridian plane. The radius of these circles and the position of their centers can depend on the polar angle. Analytical expressions for the velocity components are found near both jump surfaces. Then equations which need to be solved to get a continuous velocity field in the whole deforming material are obtained. These equations define a surface where the two solutions must match. The expression in quadratures is obtained for the upper bound on the limit load for a structure made of material obeying the von Mises yield criterion and loaded with a force acting in the z-direction of a cylindrical coordinates system. The upper bound on the limit load is determined for a tubular T-joint with the brace fixed perpendicularly to the chord of a rectangular cross section.

Introduction

Limit load solutions are convenient tool for the plastic design of different kinds of structures (see for example Baker and Heyman (1), Save and Massonnet (2), Sobotka (3), Malinin (4)). The limit load is also an important input parameter for some models in fracture mechanics, for instance for the Engineering Treatment Model proposed by Schwalbe and Cornec (5). The rigid plastic analysis is a suitable technique for obtaining limit load solutions because:

1. It was shown by Drucker and co-authors (6) that limit loads estimated, using the rigid-plastic material model, are applicable for materials which have to be assumed to be elastic-plastic.

2. More detailed analysis of beams based on the elastic-plastic material model showed that very small settlements or rotations of supposedly fixed supports can make very large differences to the computed values of the bending moments (Baker and Heyman (1), p.51). Since the exact boundary conditions cannot be satisfied in practice these solutions are not suitable for engineering applications.

A great number of investigations on the plastic design of structures are based on the concept of generalized variables introduced by Prager (7). When applied to beams, plates and shells the generalized variables (stresses and strains) usually follow from the Bernoulli's hypothesis that plane cross sections remain plane and orthogonal to the deformed material axis (Baker and Heyman (1), Save and Massonnet (2)). This assumption is accepted as a direct consequence of the fact that structure elements are thin in certain directions. For plastic design with Bernoulli's hypothesis it is also usually assumed that shear stresses do not influence yielding (Save and Massonnet (2), p.59). An important aspect in the concept of generalized variables when applied to beams, plates and shells is the fully plastic moment which results from the discontinuous stress field at a cross section where a plastic hinge appears. This moment is proportional to the tensile yield stress. The rate of internal energy dissipation at this hinge, which is needed to obtain an upper bound on the limit load, is expressed through the fully plastic moment and relative angular velocity of two coupled elements of a structure. Hence, these elements are assumed to be rigid. In this case it follows from the general theory that the rate of internal energy dissipation at the hinge, which forms the velocity discontinuity surface, should be related to the shear yield stress rather than to the tensile yield stress. In order to take this into account it is necessary to consider a kinematically admissible velocity field near the plastic hinge. Such solutions for different kinds of bending fracture specimens have been found by Ewing and Richards (8), Green (9), Hu and Albrecht (10), Lee and Parks (11) and Joch and co-authors (12). These papers also review previous research articles. All these solutions have been based on kinematically admissible velocity fields involving a single line with a velocity discontinuity ((8), (10)-(12)) or on the slip line fields (9). Thus, the first group of solutions is restricted to plane strain or plane stress conditions because more general cases would require some

deformation within a volume of the body. In the second group the characteristic method has been adopted. Since equations for non-planar deformation are not hyperbolic (except for Tresca material and sometimes for other yield criteria with the assumption of plane stress conditions) this approach cannot be extended to more general cases. In order to develop an approach based on a single line with a velocity discontinuity for axisymmetric and three dimensional deformation it is necessary to find an appropriate kinematically admissible velocity field compatible with some rigid body motions. In this paper such a kinematically admissible velocity field is proposed for axisymmetric and three dimensional deformation. This velocity field involves two velocity discontinuity surface, one is situated between the deforming material and the motionless rigid material, and the other is between the deforming material and the rigid material moving along the z-axis of a cylindrical coordinate system. These velocity discontinuity surfaces form circles on any meridian plane. The radius of these circles and the position of their centers can depend on the polar angle. Analytical expressions for the velocity components are found near both jump surfaces. Then equations which need to be solved to get a continuous velocity field in the whole deforming material are obtained. These equations also determine a surface where the two solutions must be matched. Some convenient coordinate systems are introduced for calculations of the work rate at the jump surfaces. The expression in quadratures is obtained for the upper bound on the limit load for a structure made of material obeying the von Mises yield criterion and loaded with a force acting in the z-direction of a cylindrical coordinate system. A particular velocity field is considered with the assumption that the normal vector to the interface between two material volumes, where the different analytical expressions for the velocity components are valid, has zero component in the z-direction of a cylindrical coordinate system. This velocity field is used to determine the upper bound limit load for a tubular T-joint with the chord of a rectangular cross section.

General velocity field

We first consider axisymmetric deformation without rotation in a cylindrical coordinate system rθz. In this case the only possible rigid body motion is a translation along the z-axis with a velocity v_0. Hence, a general kinematically admissible velocity field must be compatible with such a rigid body motion and with a motionless rigid zone. We assume that the intersection of a velocity discontinuity surface and a meridian plane is a rigid-plastic boundary in the shape of an arc of a circle. Let r_0 and z_0 be the coordinates of the center of this circle and ρ_0 be its radius. We begin with a rigid-plastic boundary between a motionless rigid zone and deforming material. In this case the velocity vector must have a zero normal component on the rigid- plastic boundary. It is convenient to introduce a ρφ coordinate system on a meridian plane with the following transformation equations

$$r = r_0 + \rho\cos\varphi, \quad z = z_0 + \rho\sin\varphi \tag{1}$$

In this coordinate system the equation for the jump line is $\rho = \rho_0$ with ρ_0 being a constant. Therefore, the velocity component v_ρ must vanish at $\rho = \rho_0$.

$$v_\rho = 0 \text{ at } \quad \rho = \rho_0 \tag{2}$$

On the other hand, it follows from geometrical considerations that

$$v_\rho = v_r\cos\varphi + v_z\sin\varphi \tag{3}$$

with v_r and v_z being the velocity components in the radial and axial directions respectively. We assume that condition (2) is satisfied not only at $\rho = \rho_0$ but also for the part of the body near to this surface. Then, combining (2) and (3) we obtain

$$v_r\cos\varphi + v_z\sin\varphi = 0 \tag{4}$$

The incompressibility equation in a cylindrical coordinate system has the form

$$\frac{\partial v_r}{\partial r} + \frac{\partial v_\theta}{r\partial\theta} + \frac{v_r}{r} + \frac{\partial v_z}{\partial z} = 0 \tag{5}$$

Because we consider axisymmetric deformation without rotation the velocity component v_θ=0. Therefore, it follows from (4) and (5) that

$$v_r = -v_z\tan\varphi \tag{6}$$

$$\frac{\partial v_z}{\partial z} - \tan\varphi \frac{\partial v_z}{\partial r} - v_z\left(\cos^{-2}\varphi \frac{\partial \varphi}{\partial r} + r^{-1}\tan\varphi\right) = 0 \qquad (7)$$

or in terms of the radial velocity v_r

$$\frac{\partial v_r}{\partial r} + \frac{v_r}{r} - \cot\varphi \frac{\partial v_r}{\partial z} + v_r \sin^{-2}\varphi \frac{\partial \varphi}{\partial z} = 0 \qquad (8)$$

Equation (7) can be transformed by means of (1) to the following form

$$(z - z_0)^{-1} \frac{\partial v_z}{\partial z} - (r - r_0)^{-1} \frac{\partial v_z}{\partial r} = \frac{r_0 v_z}{r(r - r_0)^2}$$

The general solution to this equation is

$$v_z = v_0 (r - r_0) r^{-1} F(\Omega) \qquad (9)$$

where $\Omega = (z - z_0)^2 + (r - r_0)^2$ and F is an arbitrary function of its argument, Ω. It follows from (1), (6) and (9) that the velocity component v_r is given by

$$v_r = -v_0 (z - z_0) r^{-1} F(\Omega) \qquad (10)$$

We now consider a rigid zone moving with velocity v_0 along the z-axis. A unit normal vector to the line $\rho = \rho_0$ on a meridian plane may be written in the following form

$$\bar{n} = \cos\varphi \bar{e}_r + \sin\varphi \bar{e}_z \qquad (11)$$

with $\bar{e}_r$ and $\bar{e}_z$ being the unit basis vectors of the cylindrical coordinate system. The velocity vector on the right side of the rigid-plastic boundary is

$$\bar{v}^{(r)} = v_0 \bar{e}_z \qquad (12)$$

From (11) and (12) we can obtain the velocity component normal to the rigid-plastic boundary

$$v_n^{(r)} = \bar{v}^{(r)} \cdot \bar{n} = v_0 \sin\varphi \qquad (13)$$

Combining (13) with the condition that the normal component of velocity must be continuous across a rigid-plastic boundary, it follows that the normal component of velocity on the deforming side of the rigid-plastic boundary is

$$v_n^{(pl)} = v_\rho = v_n^{(r)} = v_0 \sin\varphi \quad \text{at} \quad \rho = \rho_0 \qquad (14)$$

As before, we assume that velocity v_ρ satisfies equation (14) not only at $\rho = \rho_0$ but in some volume of the deforming material near to the surface $\rho = \rho_0$. Then, substitution (14) into (3) leads to

$$v_r \cos\varphi + v_z \sin\varphi = v_0 \sin\varphi$$

Transforming this equation and combining it with the incompressibility equation (5) we find that

$$v_z = v_0 - v_r \cot\varphi \tag{15}$$

$$\frac{\partial v_r}{\partial r} + \frac{v_r}{r} - \cot\varphi \frac{\partial v_r}{\partial z} + v_r \sin^{-2}\varphi \frac{\partial \varphi}{\partial z} = 0 \tag{16}$$

One can see that equation (16) is the same as equation (8) therefore the general solution (10) for the velocity component v_r is still valid, however, function of integration may be different so that

$$v_r = -v_0 (z - z_0) r^{-1} \Phi(\Omega) \tag{17}$$

where Φ is an arbitrary function of Ω. Then, it follows from (1), (15) and (17), that the velocity component v_z is given by

$$v_z = v_0 \left[1 + (r - r_0) r^{-1} \Phi(\Omega)\right] \tag{18}$$

Finally, it is necessary to match the velocity field given by (9) and (10) with that obtained from (17) and (18) to get a continuous velocity field in the whole deforming material. To this end we let $z_0 = z_a$ and $r_0 = r_a$ for the velocity field (17) and (18), and $z_0 = z_b$ and $r_0 = r_b$ for the velocity field (9) and (10). Let $r = f(z)$ be a line on a meridian plane which is the boundary between material volumes where different analytical expressions for the velocity hold. Since velocity must be continuous on the line $r = f(z)$ it follows from (9), (10) and (18) that

$$\begin{aligned}
&(z - z_b) F\left[(z - z_b)^2 + (f(z) - z_b)^2\right] = (z - z_a) \Phi\left[(z - z_a)^2 + (f(z) - z_a)^2\right] \\
&\frac{f(z) - r_b}{f(z)} F\left[(z - z_b)^2 + (f(z) - z_b)^2\right] = \\
&\qquad 1 + \frac{f(z) - r_a}{f(z)} \Phi\left[(z - z_a)^2 + (f(z) - z_a)^2\right]
\end{aligned} \tag{19}$$

Thus, if function $f(z)$ is prescribed then equations (19) define the functions F and Φ. Then, by means of (9), (10), (17) and (18) the continuous velocity field in the whole deforming

material can be obtained. Generally, the function f(z) can be determined by minimizing the functional following from the upper bound theorem.

Up to now we have dealt with the axisymmetric velocity field. However, it is easy to show by substitution of (9), (10) and (17), (18) into (5) that the velocity fields are still solenoidal if z_0 and r_0 are functions of θ, and F and Φ are functions of Ω and θ (Ω is given by the different expressions near each velocity discontinuity surface). This leads to nonaxisymmetric kinematically admissible velocity fields. In this case f can be function of z and θ. In order to obtain the equation describing the jump surface, $\Sigma = 0$, for a nonaxisymmetric velocity field we introduce the components of the gradient vector to this surface in the cylindrical coordinates as follows

$$\mathrm{grad}_r\Sigma = \partial\Sigma/\partial r, \quad \mathrm{grad}_\theta\Sigma = r^{-1}\,\partial\Sigma/\partial\theta, \quad \mathrm{grad}_z\Sigma = \partial\Sigma/\partial z \tag{20}$$

On the rigid-plastic boundary between the motionless rigid zone and the deforming material, Σ_b, the equation $v_r\mathrm{grad}_r\Sigma_b + v_z\mathrm{grad}_z\Sigma_b = 0$ is to be satisfied that, by means of (9), (10) and (20), results in

$$(r - r_b)\partial\Sigma_b/\partial z - (z - z_b)\partial\Sigma_b/\partial r = 0$$

which can be integrated to give

$$\Sigma_b = (r - r_b)^2 + (z - z_b)^2 - \rho_b^2 = 0 \tag{21}$$

where ρ_b is an arbitrary function of θ. On the rigid-plastic boundary between the moving rigid zone and the deforming material, Σ_a, we have

$$v_r\mathrm{grad}_r\Sigma_a + v_z\mathrm{grad}_z\Sigma_a = v_0\mathrm{grad}_z\Sigma_a$$

By means of (17), (18) and (20) this equation transforms to

$$(r - r_a)\partial\Sigma_a/\partial z - (z - z_a)\partial\Sigma_a/\partial r = 0$$

which leads to

$$\Sigma_a = (r - r_a)^2 + (z - z_a)^2 - \rho_a^2 = 0 \tag{22}$$

where ρ_a is an arbitrary function of θ. It follows from (21) and (22) that the intersection of the jump surface Σ_a with any meridian plane is a circle of radius ρ_b with its center at the point given by $r = r_b$ and $z = z_b$. For the jump surface Σ_a these values are ρ_a, r_a, and z_a respectively.

Plastic work rate

It is necessary to take into account the energy dissipated at the two jump surfaces and within the deforming material. Let k be the shear yield stress and v_τ be the component of the velocity tangent to the jump surface then the work rate at a velocity discontinuity surface is given by

$$\dot{w}_d = k\iint \left[\!\left[v_\tau \right]\!\right] d\Sigma \tag{23}$$

with the usual square brackets notation for the amount of jump. It is convenient to use an infinitesimal surface element $d\Sigma$ in the coordinate system $\rho\theta\varphi$. From geometrical considerations it is clear that

$$d\Sigma \sqrt{\text{grad}_r^2 \Sigma + \text{grad}_z^2 \Sigma} \Big/ \left|\text{grad}\Sigma\right| = \rho_0 r d\varphi d\theta \tag{24}$$

where the value of r corresponds to points on the jump surface. The components of the gradient vector and its magnitude can be found from (20) using (21) and (22). Then expression (24) for the Σ_a surface transforms to

$$d\Sigma_a = \sqrt{r^2\rho_a^2 + \left[(r - r_a)da/d\theta + (z - z_a)dz_a/d\theta + \rho_a d\rho_a/d\theta\right]^2}\, d\varphi d\theta$$

which further transforms when combined with (1) assuming that $\rho = \rho_a$ to

$$d\Sigma_a = \rho_a \sqrt{(r_a + \cos\varphi)^2 + \left[\cos\varphi dr_a/d\theta + \sin\varphi dz_a/d\theta + d\rho_a/d\theta\right]^2}\, d\varphi d\theta \tag{25}$$

Analogously, for the jump surface Σ_b we have

$$d\Sigma_b = \rho_b \sqrt{(r_b + \cos\varphi)^2 + \left[\cos\varphi dr_b/d\theta + \sin\varphi dz_b/d\theta + d\rho_b/d\theta\right]^2}\, d\varphi d\theta \tag{26}$$

The amount of velocity jump on the surface Σ_b can be found from (9) and (10) as follows

$$\left[\!\left[v_\tau \right]\!\right] = \sqrt{v_r^2 + v_z^2} = v_0 r^{-1} \left|F(\Omega)\right| \sqrt{(r - r_b)^2 + (z - z_b)^2}$$

which, when (1) and (21) are substituted, transforms to

$$\left[\!\left[v_\tau \right]\!\right] = v_0 (r_b + \rho_b \cos\varphi)^{-1} \left|F(\rho_b^2)\right| \rho_b \tag{27}$$

Substitution of (26) and (27) into (23) gives the magnitude of the rate of internal energy dissipation at the Σ_b surface

$$\dot{w}_{db} = kv_0 \times$$

$$\iint \frac{\rho_b^2 \left|F\left(\rho_b^2\right)\right|}{\left(r_b + \rho_b \cos\varphi\right)} \sqrt{\left(r_b + \rho_b \cos\varphi\right)^2 + \left(\cos\varphi \frac{dr_b}{d\theta} + \sin\varphi \frac{dz_b}{d\theta} + \frac{d\rho_b}{d\theta}\right)^2} \, d\varphi d\theta \quad (28)$$

On the jump surface Σ_a we have $\left[\left[v_\tau\right]\right] = \sqrt{v_r^2 + \left(v_z - v_0\right)^2}$ and it follows from (17) and (18) that

$$\left[\left[v_\tau\right]\right] = v_0 r^{-1} \left|\Phi(\Omega)\right| \sqrt{\left(z - z_0\right)^2 + \left(r - r_0\right)^2}$$

The further transformations due to (1) and (22) lead to

$$\left[\left[v_\tau\right]\right] = v_0 \left(r_a + \rho_a \cos\varphi\right)^{-1} \left|\Phi\left(\rho_a^2\right)\right| \rho_a \quad (29)$$

Substitution of (25) and (29) into (23) gives the magnitude of the rate of internal energy dissipation at the Σ_a surface

$$\dot{w}_{da} = kv_0 \times$$

$$\iint \frac{\rho_a^2 \left|\Phi\left(\rho_a^2\right)\right|}{\left(r_a + \rho_a \cos\varphi\right)} \sqrt{\left(r_a + \rho_a \cos\varphi\right)^2 + \left(\cos\varphi \frac{dr_a}{d\theta} + \sin\varphi \frac{dz_a}{d\theta} + \frac{d\rho_a}{d\theta}\right)^2} \, d\varphi d\theta \quad (30)$$

For axisymmetric deformation the derivatives vanish in expressions (28) and (30) therefore in this case we have

$$\dot{w}_{da} = kv_0 \rho_a^2 \left|\Phi\left(\rho_a^2\right)\right| \iint d\varphi d\theta, \quad \dot{w}_{db} = kv_0 \rho_b^2 \left|F\left(\rho_b^2\right)\right| \iint d\varphi d\theta \quad (31)$$

The limits of integration in (28), (30) and (31) have to be determined from geometrical considerations for a specific structure. A possible geometry of the deforming body, rigid zones and coordinate systems are shown in Fig.1. Functions $z_l(r,\theta)$ and $z_u(r,\theta)$ are known since they are defined by geometry of the structure. At any value of θ, the φ coordinates of points A, B, C and D in the $\rho\theta\varphi$ coordinate system, φ_A, φ_B, φ_C and φ_D can be found from the following transcendental equations

$$
\begin{aligned}
z_l\left(r_a+\rho_a\cos\varphi_A,\theta\right)&=z_a+\rho_a\sin\varphi_A\\
z_l\left(r_b+\rho_b\cos\varphi_C,\theta\right)&=z_b+\rho_b\sin\varphi_A\\
z_u\left(r_a+\rho_a\cos\varphi_B,\theta\right)&=z_a+\rho_a\sin\varphi_B\\
z_l\left(r_b+\rho_b\cos\varphi_D,\theta\right)&=z_b+\rho_b\sin\varphi_D
\end{aligned}
\tag{32}
$$

The solution to these equations defines the limits with respect to φ of the integrals in (28) and (30) which, then, can be transformed to

$$
\begin{aligned}
&\dot{w}_{db}=kv_0\times\\
&\int_0^{2\pi}\rho_b^2\left|F\left(\rho_b^2\right)\right|\int_{\varphi_D(\theta)}^{\varphi_C(\theta)}\sqrt{1+\left(r_b+\rho_b\cos\varphi\right)^{-2}\left[\cos\varphi\frac{dr_b}{d\theta}+\sin\varphi\frac{dz_b}{d\theta}+\frac{d\rho_b}{d\theta}\right]^2}\,d\varphi d\theta\\
&\dot{w}_{da}=kv_0\times\\
&\int_0^{2\pi}\rho_a^2\left|\Phi\left(\rho_a^2\right)\right|\int_{\varphi_A(\theta)}^{\varphi_B(\theta)}\sqrt{1+\left(r_a+\rho_a\cos\varphi\right)^{-2}\left[\cos\varphi\frac{dr_a}{d\theta}+\sin\varphi\frac{dz_a}{d\theta}+\frac{d\rho_a}{d\theta}\right]^2}\,d\varphi d\theta
\end{aligned}
\tag{33}
$$

In an axisymmetric case, integration with respect to φ in expressions (31) can be carried out to give

$$
\begin{aligned}
\dot{w}_{da}&=kv_0\rho_a^2\left|\Phi\left(\rho_a^2\right)\right|\int_0^{2\pi}\left[\varphi_B(\theta)-\varphi_A(\theta)\right]d\theta,\\
\dot{w}_{db}&=kv_0\rho_b^2\left|F\left(\rho_b^2\right)\right|\int_0^{2\pi}\left[\varphi_C(\theta)-\varphi_D(\theta)\right]d\theta
\end{aligned}
\tag{34}
$$

(The limits with respect to θ are not necessarily from 0 to 2π but also determined by the geometry of the structure. However, we restrict our studies to problems which require the limits from 0 to 2π because the limits for other structures can be obtained from simple geometrical considerations). We adopt the von Mises yield criterion. In this case the work rate within the deforming material is given by

$$
\dot{w}_V=k\iiint_{V_1}\sqrt{2\dot{\varepsilon}_{ij}\dot{\varepsilon}_{ij}}\,dV+k\iiint_{V_2}\sqrt{2\dot{\varepsilon}_{ij}\dot{\varepsilon}_{ij}}\,dV
\tag{35}
$$

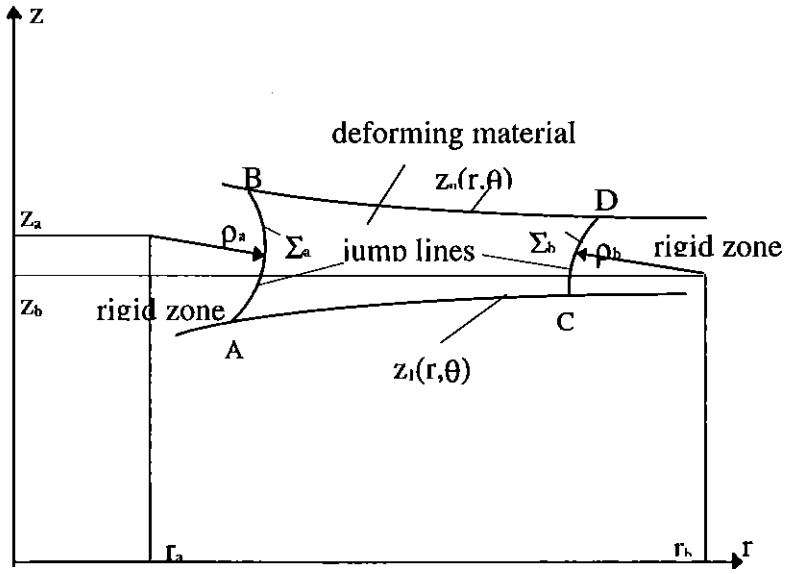

Fig.1 Possible geometry of the deforming body.

Here V_1 is the material volume where velocity field (9) and (10) is valid and V_2 is the material volume where velocity field (17) and (18) is valid, and $\dot{\varepsilon}_{ij}$ are the components of the strain rate tensor which can be calculated from (9), (10) and (17), (18) respectevely. In the cylindrical coordinates we have

$$\dot{\varepsilon}_r = -\frac{v_0(z-z_b)}{r^2}\left[2r(r-r_b)\frac{\partial F}{\partial \Omega} - F\right], \quad \dot{\varepsilon}_z = \frac{2v_0(r-r_b)(z-z_b)}{r}\frac{\partial F}{\partial \Omega}$$

$$\dot{\varepsilon}_\theta = -\frac{v_0(z-z_b)}{r^2}F,\ 2\dot{\varepsilon}_{rz} = \frac{v_0}{r}\left\{\left(\frac{r_b}{r}-1\right)F + 2\left[(r-r_b)^2 - (z-z_b)^2\right]\frac{\partial F}{\partial \Omega}\right\}$$

$$2\dot{\varepsilon}_{r\theta} = \frac{v_0}{r^2}\left\{F\frac{dz_b}{d\theta} + (z-z_b)\frac{\partial F}{\partial \Omega}\left[2(z-z_b)\frac{dz_b}{d\theta} + 2(r-r_b)\frac{dr_b}{d\theta} - 1\right]\right\} \qquad (36)$$

$$2\dot{\varepsilon}_{z\theta} = -\frac{v_0}{r^2}\left\{F\frac{dr_b}{d\theta} + (r-r_b)\frac{\partial F}{\partial \Omega}\left[2(z-z_b)\frac{dz_b}{d\theta} + 2(r-r_b)\frac{dr_b}{d\theta} - 1\right]\right\}$$

for velocity field (9) and (10) and

$$\dot{\varepsilon}_r = -\frac{v_0(z-z_a)}{r^2}\left[2r(r-r_a)\frac{\partial \Phi}{\partial \Omega} - \Phi\right], \quad \dot{\varepsilon}_z = \frac{2v_0(r-r_a)(z-z_a)}{r}\frac{\partial \Phi}{\partial \Omega}$$

$$\dot{\varepsilon}_\theta = -\frac{v_0(z-z_a)}{r^2}\Phi,\ 2\dot{\varepsilon}_{rz} = \frac{v_0}{r}\left\{\left(\frac{r_a}{r}-1\right)\Phi + 2\left[(r-r_a)^2-(z-z_a)^2\right]\frac{\partial\Phi}{\partial\Omega}\right\}$$

$$2\dot{\varepsilon}_{r\theta} = \frac{v_0}{r^2}\left\{\Phi\frac{dz_a}{d\theta} + (z-z_a)\frac{\partial\Phi}{\partial\Omega}\left[2(z-z_a)\frac{dz_a}{d\theta} + 2(r-r_a)\frac{dr_a}{d\theta} - 1\right]\right\} \qquad (37)$$

$$2\dot{\varepsilon}_{z\theta} = -\frac{v_0}{r^2}\left\{\Phi\frac{dr_a}{d\theta} + (r-r_a)\frac{\partial\Phi}{\partial\Omega}\left[2(z-z_a)\frac{dz_a}{d\theta} + 2(r-r_a)\frac{dr_a}{d\theta} - 1\right]\right\}$$

for velocity field (17) and (18). For axisymmetric deformation all derivatives with respect to θ in (36) and (37) vanish. The total internal energy dissipation rate for the structure shown in Fig.1 is determined as

$$\dot{W}_i = \dot{W}_V + \dot{W}_{db} + \dot{W}_{da} \qquad (38)$$

If the surface $z_l(r, \theta)$ and $z_u(r, \theta)$ are stress free and an external force, P, is applied to the moving rigid material in the z-direction then the work rate of external forces is given by

$$\dot{W}_e = Pv_0 \qquad (39)$$

The upper bound on the limit load, P_u, is determined from the equation $\dot{W}_e = \dot{W}_i$. This, combined with (38) and (39), results in

$$P_u = v_0^{-1}\left(\dot{W}_V + \dot{W}_{db} + \dot{W}_{da}\right) \qquad (40)$$

where $\dot{W}_{db}$ and $\dot{W}_{da}$ are determined from (33) and $\dot{W}_V$ from (35) with the use of (36) and (37).

Particular velocity field

As a particular case we will consider the function $f(z) = r_m$ in (19) with r_m being a function of θ. In this case equation (19) are satisfied by

$$z_a = z_b = z_0 \quad \text{and} \quad F = \Phi = F_0 \qquad (41)$$

where

$$F_0 = r_m/(r_a - r_b) \qquad (42)$$

Now we are able to define the velocity field near the motionless rigid zone by means of (9), (10), (41) and (42)

$$v_z = v_0 \frac{(r - r_b)r_m}{(r_a - r_b)r}, \quad v_r = -v_0 \frac{(z - z_0)r_m}{(r_a - r_b)r} \tag{43}$$

and near the moving rigid zone by means of (17), (18), (41) and (42)

$$v_z = v_0 \left[1 + \frac{(r - r_a)r_m}{(r_a - r_b)r} \right], \quad v_r = -v_0 \frac{(z - z_0)r_m}{(r_a - r_b)r} \tag{44}$$

Both (43) and (44) give a continuous velocity field in the whole deforming material. With these velocity fields expressions (36) and (37) are simplified to the following

$$\dot{\varepsilon}_r = \frac{v_0(z - z_0)r_m}{(r_a - r_b)r^2}, \quad \dot{\varepsilon}_z = 0, \quad \dot{\varepsilon}_\theta = -\frac{v_0(z - z_0)r_m}{(r_a - r_b)r^2}$$

$$2\dot{\varepsilon}_{rz} = \frac{v_0 r_m}{(r_a - r_b)r}\left(\frac{r_b}{r} - 1\right)$$

$$2\dot{\varepsilon}_{r\theta} = \frac{v_0 r_m}{(r_a - r_b)r^2}\left\{\frac{dz_0}{d\theta} - (z - z_0)\frac{d\ln\left[r_m/(r_a - r_b)\right]}{d\theta}\right\} \tag{45}$$

$$2\dot{\varepsilon}_{z\theta} = -\frac{v_0 r_m}{(r_a - r_b)r^2}\left\{\frac{dr_b}{d\theta} - (r - r_b)\frac{d\ln\left[r_m/(r_a - r_b)\right]}{d\theta}\right\}$$

in the case of velocity field (43) and

$$\dot{\varepsilon}_r = \frac{v_0(z - z_0)r_m}{(r_a - r_b)r^2}, \quad \dot{\varepsilon}_z = 0, \quad \dot{\varepsilon}_\theta = -\frac{v_0(z - z_0)r_m}{(r_a - r_b)r^2}$$

$$2\dot{\varepsilon}_{rz} = \frac{v_0 r_m}{(r_a - r_b)r}\left(\frac{r_a}{r} - 1\right)$$

$$2\dot{\varepsilon}_{r\theta} = \frac{v_0 r_m}{(r_a - r_b)r^2}\left\{\frac{dz_0}{d\theta} - (z - z_0)\frac{d\ln\left[r_m/(r_a - r_b)\right]}{d\theta}\right\} \tag{46}$$

$$2\dot{\varepsilon}_{z\theta} = -\frac{v_0 r_m}{(r_a - r_b)r^2}\left\{\frac{dr_a}{d\theta} - (r - r_a)\frac{d\ln\left[r_m/(r_a - r_b)\right]}{d\theta}\right\}$$

in the case of velocity field (44). Substitution of (41) and (42) into (33) gives the rate of energy dissipation at the jump surfaces as

$$\dot{w}_{db} = kv_0 \times$$
$$\int_0^{2\pi} \frac{\rho_b^2 r_m}{r_b - r_a} \int_{\varphi_D(\theta)}^{\varphi_C(\theta)} \sqrt{1 + (r_b + \rho_b \cos\varphi)^{-2} \left[\cos\varphi \frac{dr_b}{d\theta} + \sin\varphi \frac{dz_0}{d\theta} + \frac{d\rho_b}{d\theta} \right]^2} \, d\varphi d\theta$$
$$\dot{w}_{da} = kv_0 \times \tag{47}$$
$$\int_0^{2\pi} \frac{\rho_b^2 r_m}{r_b - r_a} \int_{\varphi_A(\theta)}^{\varphi_B(\theta)} \sqrt{1 + (r_a + \rho_a \cos\varphi)^{-2} \left[\cos\varphi \frac{dr_a}{d\theta} + \sin\varphi \frac{dz_0}{d\theta} + \frac{d\rho_a}{d\theta} \right]^2} \, d\varphi d\theta$$

Using (45) and (46) the rate of energy dissipation within the deforming material can be obtained from (35) by direct substitutions.

Limit load for tubular T-joints

We apply the particular velocity field given in the previous section to determine an upper bound limit load for tubular T-joints with the chord of a rectangular cross section (Fig.2). Taking into account geometry of the structure it is natural to assume that

$$z_0 = 0,\ \rho_a = \rho_b = h/2 \text{ and } r_a = R \tag{48}$$

where h is the thickness of the chord wall and R is the outer radius of the brace. We first apply the axisymmetric velocity field. Then, r_b and r_m are constants and should be determined from the upper bound theorem. Combining (35), (40), (45)-(48) gives

$$P^* = \pi \left(\frac{1 + h^*}{r_b^* - 1} \right) \times$$
$$\left[\int_0^{h^*/2} \int_{r_m^*}^{r_2} \sqrt{\frac{4z^2}{r^2} + \left(\frac{r_b^*}{r} - 1 \right)^2} \, dr dz + \int_0^{h^*/2} \int_{r_1}^{r_m^*} \sqrt{\frac{4z^2}{r^2} + \left(\frac{1}{r} - 1 \right)^2} \, dr dz + \pi h^{*2} \right] \tag{49}$$

where $r_2 = r_b^* - \sqrt{h^{*2}/4 - z^2}$ and $r_1 = 1 + \sqrt{h^{*2}/4 - z^2}$. We have introduced here the dimensionless quantities $P^* = P_u / 4kR^2$, $h^* = h/R$, $r_b^* = r_b/R$, $r_m^* = r_m/R$.

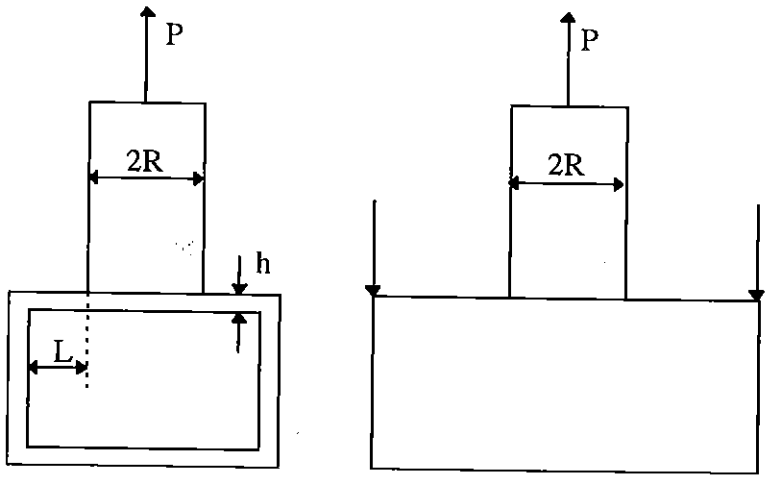

Fig.2 Shape of the tubular T-joint

Expression (49) has been minimized numerically with respect to r_m^* and r_b^*. The value of r_m^* is given by

$$r_m^* = 1 + h^*/2 \tag{50}$$

Variation of P^* and r_b^* with h^* are shown in Fig. 3 and Fig.4 respectively. This solution holds if

$$r_b \le R + L \quad \left(r_b^* \le 1 + L^*\right) \tag{51}$$

where $L^* = L/R$ (see Fig.2 for definition for L). If this inequality is not satisfied, that can be checked for any specific structure using Fig.4, than nonaxisymmetric velocity field should lead to a better upper bound. We assume that (48) and (50) are still valid for such nonaxisymmetric velocity field. Moreover, we assume that the curve $r_b^* = r_b^*(\theta)$ is an ellipse given by the following equation

$$r_b^* = a^*\left(1 + L^*\right) \Big/ \sqrt{\left(1 + L^*\right)^2 \cos^2\theta + a^{*2} \sin^2\theta} \tag{52}$$

With these assumptions expression (40) can be transformed to

$$P^* = \frac{P_u}{4kR^2} =$$

$$2\int_0^{\pi/2}\int_0^{h^*/2}\int_{r_m^*}^{r_2}\left(\frac{1+h^*}{r_b^*-1}\right)\sqrt{\frac{4z^2}{r^2}+\left(\frac{r_b^*}{r}-1\right)^2+\frac{z^2+(1-r)^2}{r^2\left(1-r_b^*\right)^2}\left(\frac{dr_b^*}{d\theta}\right)^2}\,drdzd\theta +$$

$$2\int_0^{\pi/2}\int_0^{h^*/2}\int_{r_1}^{r_m^*}\left(\frac{1+h^*}{r_b^*-1}\right)\sqrt{\frac{4z^2}{r^2}+\left(\frac{1}{r}-1\right)^2+\frac{z^2+(1-r)^2}{r^2\left(1-r_b^*\right)^2}\left(\frac{dr_b^*}{d\theta}\right)^2}\,drdzd\theta + \qquad (53)$$

$$2h^{*2}\int_0^{\pi/2}\left(\frac{1+h^*}{r_b^*-1}\right)\int_{\pi/2}^{\pi}\sqrt{1+\frac{\cos^2\varphi}{\left(r_b^*+h^*\cos\varphi\right)^2}\left(\frac{dr_b^*}{d\theta}\right)^2}\,d\varphi d\theta + h^{*2}\pi\int_0^{\pi/2}\frac{1+h^*}{r_b^*-1}d\theta$$

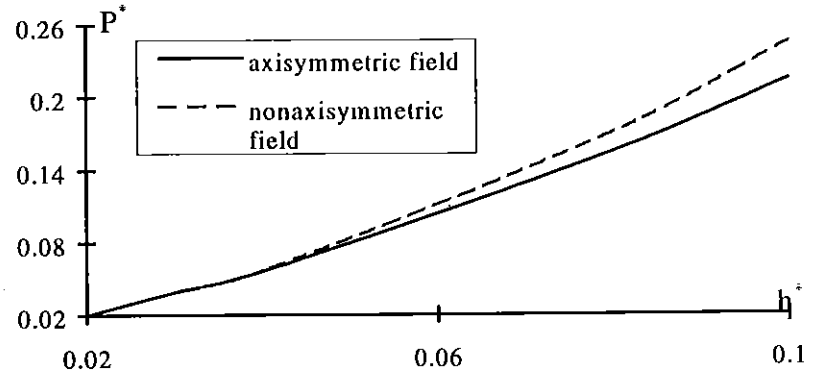

Fig.3 Variation of the limit load with h*.

The equations for r_1 and r_2 given after (49) are still valid, however, r_2 depends here on z and θ since r_b^* depends on θ. r_b^* and $dr_b^*/d\theta$ are determined from (52) with a^* being a constant which should be calculated from the upper bound theorem. As an example we take $L^* = 0.5$. In this case it follows from Fig.4 and inequality (51) that the axisymmetrical solution is applicable for $h^* \leq 0.03$. For $h^* > 0.03$ the upper bound has been obtained by minimizing (53) with respect to a^*. Variation of the upper bound and the a^* value, which determines the size of the plastic zone, with h^* are shown in Fig.3 and Fig.4 respectively. One can see from Fig.3 that the limit load based on the nonaxisymmetric velocity field is

higher than that based on the axisymmetric velocity field. However we should note that for the example the solution based on the axisymmetric velocity field is not valid for $h^* > 0.03$.

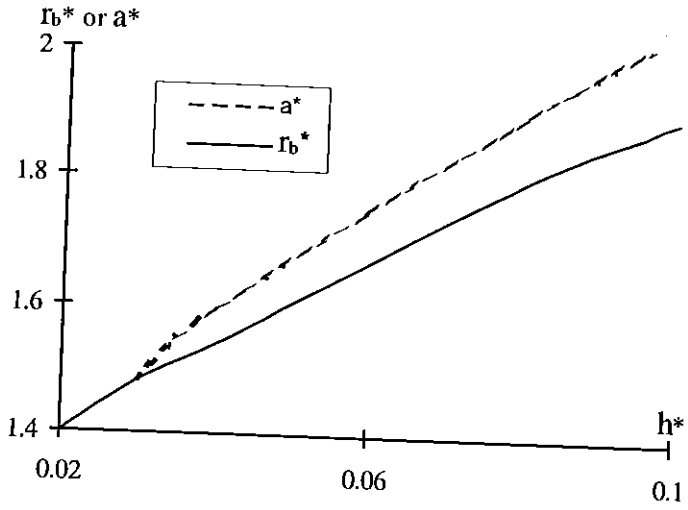

Fig.4 Variation of the size of the plastic zone with h*.

Conclusion

Axisymmetric and nonaxisymmetric kinematically admissible velocity fields involving two velocity discontinuity surfaces are proposed. Expressions in quadratures for the limit load are given. The upper bound limit load based on the proposed velocity fields is found for tubular T-joints with the chord of a rectangular cross section. For thin walled structures the axisymmetric velocity field leads to a better upper bound. This solution holds if inequality (51) is satisfied. Using Fig.4 this inequality can be checked for any specific structure. The nonaxisymmetric velocity field with the elliptic plastic hinge is used to obtain the limit load for structure, for which the inequality is not satisfied.

References

(1) BAKER L. and HEYMAN J., (1980), Plastic Design of Frames. 1. Fundamentals, Cambridge University Press, Cambridge.

(2) SAVE M.A. and MASSONET C.E., (1972), Plastic Analysis and Design of Plates, Shells and Disks, North-Holland Publishing Company, Amsterdam.

(3) SOBOTKA Z., (1989), Theory of Plasticity and Limit Design of Plates, Elsevier, Amsterdam.

(4) MALININ N.N., (1975), Applied Theory of Plasticity and Creep, Maschinostroenie, Moscow (in Russian).

(5) SCHWALBE K.-H. and CORNEC A., (1991), The Engineering Treatment Model (ETM) and Its Practical Application, Fatigue Fract. Engng Mater. Struct., vol. 14, pp.405-412.

(6) DRUCKER D.C., PRAGER W. and GREENBERG H.J., (1952), Extended Limit Design Theorems for Continuous Media, Quart. Appl. Math., vol. 9, pp. 381-389.

(7) PRAGER W., Discontinuous Fields of Plastic Stress and Flow, Proc. Second U.S. Nat. Congr. Appl. Mech., (Ed. by P.M.Naghdi), ASME, New York, pp. 21-32.

(8) EWING D.J.F. and RICHARDS C.E., (1974), The Yield-Point of Singly-Notched Pin-Loaded Tensile Strips, J. Mech. And Phys. Solids, vol. 22, pp. 27-36.

(9) GREEN A.P., (1956), The Plastic Yielding of Shallow Notched Bars Due to Bending, J. Mech. Phys. Solids, vol. 4, pp. 259-268.

(10) HU J.M. and ALBRECHT P., (1991), Limit Load Solution and Loading Behavior of C(T) Fracture Specimen, Int. J. Fracture, vol. 52, pp. 619-645.

(11) LEE H. and PARKS D.M., (1993), Fully Plastic Analyses of Plane Strain Single-Edge-Cracked Specimens Subject to Combined Tension and Bending, Int. J. Fracture, vol. 63, pp. 329-350.

(12) JOCH J. , AINSWORTH R.A. and HYDE T.H. (1993), Limit Load and J-estimates for Idealizied Problems of Deeply Cracked Welded Joints in Plane-Strain Bending and Tension, Fatigue Fract. Engng Mater. Struct., vol. 16, pp. 1061-1080.

Acknowledgments: This work was supported in part through the Russian Foundation for Fundamental Research (Grant N^0 96-01-05017). One of the authors, S. A., would like to acknowledge Dr. U. Zerbst (GKSS Research Centre, Germany) for stimulating discussions on the potential application of these results. The authors would like to acknowledge Dr. J. Paul for his help with English.